

## BRIEF COMMUNICATION

# Dissociation Between Brown Adipose Tissue $^{18}\text{F}$ -FDG Uptake and Thermogenesis in Uncoupling Protein 1–Deficient Mice

Mohammed K. Hankir<sup>1</sup>, Mathias Kranz<sup>2</sup>, Susanne Keipert<sup>3</sup>, Juliane Weiner<sup>4</sup>, Sille G. Andreasen<sup>1</sup>, Matthias Kern<sup>1</sup>, Marianne Patt<sup>5</sup>, Nora Klötting<sup>1</sup>, John T. Heiker<sup>4</sup>, Peter Brust<sup>2</sup>, Swen Hesse<sup>1,5</sup>, Martin Jastroch<sup>\*3</sup>, and Wiebke K. Fenske<sup>\*1</sup>

<sup>1</sup>Integrated Research and Treatment Centre for Adiposity Diseases, Department of Medicine, University of Leipzig, Leipzig, Germany;

<sup>2</sup>Institute of Radiopharmaceutical Cancer Research, Department of Neuroradiopharmaceuticals, Helmholtz Centre Dresden-Rossendorf,

Leipzig, Germany; <sup>3</sup>Helmholtz Diabetes Center, Helmholtz Center Munich, Neuherberg, Germany; <sup>4</sup>Collaborative Research Center for Obesity Mechanisms, University of Leipzig, Leipzig, Germany; and <sup>5</sup>Department of Nuclear Medicine, Leipzig University Hospital, Leipzig, Germany

$^{18}\text{F}$ -FDG PET imaging is routinely used to investigate brown adipose tissue (BAT) thermogenesis, which requires mitochondrial uncoupling protein 1 (UCP1). It remains uncertain, however, whether BAT  $^{18}\text{F}$ -FDG uptake is a reliable surrogate measure of UCP1-mediated heat production. **Methods:** UCP1 knockout (KO) and wild-type (WT) mice housed at thermoneutrality were treated with the selective  $\beta_3$  adrenergic receptor agonist CL 316, 243 and underwent metabolic cage, infrared thermal imaging and  $^{18}\text{F}$ -FDG PET/MRI experiments. Primary brown adipocytes were additionally examined for their bioenergetics by extracellular flux analysis as well as their uptake of 2-deoxy- $^3\text{H}$ -glucose. **Results:** In response to CL 316, 243 treatments, oxygen consumption, and BAT thermogenesis were diminished in UCP1 KO mice, but BAT  $^{18}\text{F}$ -FDG uptake was fully retained. Isolated UCP1 KO brown adipocytes exhibited defective induction of uncoupled respiration whereas their glycolytic flux and 2-deoxy- $^3\text{H}$ -glucose uptake rates were largely unaffected. **Conclusion:** Adrenergic stimulation can increase BAT  $^{18}\text{F}$ -FDG uptake independently of UCP1 thermogenic function.

**Key Words:** animal imaging; neuroendocrine; PET/MRI; brown adipose tissue; glucose metabolism; thermogenesis; uncoupling protein 1

**J Nucl Med 2017; 58:1100–1103**  
DOI: 10.2967/jnumed.116.186460

In human PET imaging studies, brown adipose tissue (BAT)  $^{18}\text{F}$ -FDG uptake has been shown to be markedly increased by controlled cold exposure (1,2) and agonism of  $\beta_3$  adrenergic receptors (3), correlating positively with changes in energy expenditure (1,3). Similar findings have been made in small-animal PET imaging studies performed on mice (4,5).

Mitochondrial uncoupling protein 1 (UCP1) endows both human and mouse brown adipocytes with thermogenic capacity (6). It is widely assumed that BAT  $^{18}\text{F}$ -FDG uptake provides an indirect quantitative measure of thermogenesis. We therefore sought to formally test this basic assumption by performing  $^{18}\text{F}$ -FDG PET/MRI

experiments on UCP1-deficient mice that exhibit defective BAT thermogenesis and uncoupled respiration in response to the selective  $\beta_3$  adrenergic receptor agonist CL 316, 243 (7,8).

## MATERIALS AND METHODS

### Animals

Experiments were performed on female wild-type (WT) C57BL/6J mice and UCP1 knockout (KO) littermates (Jackson Laboratory) aged 3–9 mo and were all approved by the Institutional Animal Care and Use Committee at the University of Leipzig (TVV 63/13 and TVV 04/12). Animals were housed in an incubator (Memmert GmbH & Co. KG) set at thermoneutrality (30°C) and 60% humidity on a 12-h light–dark cycle and had free access to a high-fat high-sugar diet (Sniff GmbH) to potentiate thermogenic responses to adrenergic stimulation (8) unless otherwise indicated. In line with the findings of Feldmann et al. (8), UCP1 KO mice housed under these conditions consistently showed higher body weights than WT littermates (Table 1).

### Indirect Calorimetry

Animals were transferred to metabolic cages (TSE Systems) immediately after intraperitoneal injection of the selective  $\beta_3$  adrenergic receptor agonist CL 316, 243 (1 mg/kg) (Tocris) (7), and oxygen consumption was measured for 3 h by indirect calorimetry.

### Core Body Temperature Measurements

Core body temperature was measured using a rectal probe (Thermalert) at baseline and at 15-min intervals for 1 h after intraperitoneal injection of CL 316, 243 (1 mg/kg) (7).

### Infrared Thermal Imaging

Infrared thermal imaging (9) was performed using a VarioCAM thermal camera (InfraTec GmbH). Each mouse was placed on a cage top at a fixed distance away from the camera lens. Serial 1-s images (10 Hz) were taken in triplicate at baseline and at 15-min intervals for 1 h after intraperitoneal injection of CL 316, 243 (1 mg/kg). For analysis, a constantly sized circular region of interest was drawn over BAT, and the average temperature was recorded.

### PET/MRI

Small-animal PET/MRI (Mediso Medical Imaging Systems) was performed as previously described (10). Overnight fasted mice received intraperitoneal injections of either CL 316, 243 (1 mg/kg) (4) or 0.9% saline along with an intraperitoneal injection of  $18.8 \pm 0.4$  MBq of  $^{18}\text{F}$ -FDG (Department of Nuclear Medicine, University Hospital Leipzig). Animals were then returned to their home cages for 45 min and subsequently anesthetized with isoflurane (1.8%, 0.35 L/min) delivered in a 60% oxygen–40% air mixture (MCQ Instruments) and transferred to the PET/MRI scanner. A 15-min static PET scan

Received Nov. 2, 2016; revision accepted Dec. 16, 2016.

For correspondence or reprints contact: Wiebke Fenske, Integrated Research and Treatment Centre for Adiposity Diseases, Department of Medicine, University of Leipzig, Liebigstrasse 21, 04103 Leipzig, Germany.

E-mail: [WiebkeKristin.Fenske@medizin.uni-leipzig.de](mailto:WiebkeKristin.Fenske@medizin.uni-leipzig.de)

\*Contributed equally to this work.

Published online Jan. 12, 2017.

COPYRIGHT © 2017 by the Society of Nuclear Medicine and Molecular Imaging.

**TABLE 1**  
Weight of UCP1 KO Mice Compared with Their WT Littermates at Time of Experiments

Measurement	WT body weight (g)	UCP1 KO body weight (g)	<i>P</i>
Indirect calorimetry	25.3 ± 0.5 ( <i>n</i> = 3)	29.3 ± 0.3 ( <i>n</i> = 4)	0.0006
Rectal measurement	23.8 ± 0.3 ( <i>n</i> = 4)	27.3 ± 0.6 ( <i>n</i> = 5)	0.0023
Thermal imaging	25.3 ± 0.5 ( <i>n</i> = 4)	28.3 ± 0.3 ( <i>n</i> = 4)	0.0014
PET/MRI (saline)	20.6 ± 0.2 ( <i>n</i> = 4)	24.3 ± 0.8 ( <i>n</i> = 4)	0.0014
PET/MRI (CL 316, 243)	20.3 ± 0.8 ( <i>n</i> = 5)	24.5 ± 0.4 ( <i>n</i> = 5)	0.0015

Values are mean ± SEM. *P* values were obtained from unpaired 2-tailed *t* tests.

was initiated, during which animals were maintained at 37°C under isoflurane anesthesia. For analysis, mean SUVs of <sup>18</sup>F-FDG by BAT were calculated.

### Cellular Bioenergetics and 2-Deoxy-<sup>3</sup>H-Glucose Assay

Stromal vascular cells were isolated from interscapular BAT and differentiated as previously described (11). On day 7 of differentiation, mature brown adipocytes were washed twice with assay medium (XF Dulbecco modified Eagle medium supplemented with 25 mM glucose, 2 mM pyruvate, and 4% bovine serum albumin [w/v]), followed by incubation at 37°C without CO<sub>2</sub> for 20 min. Cells were transferred to an XF96 Extracellular Flux Analyzer (Seahorse Bioscience), and after 5 basal values oligomycin (5 μg/mL) was injected to induce uncoupled respiration followed by an injection of 100 μM 2,4-dinitrophenol. To correct for nonmitochondrial respiration and nonglycolytic sources of changes in extracellular acidification rate, a cocktail of 2.5 μM rotenone, 2.5 μM antimycin A, and 2.5 μM 2-deoxyglucose was injected. For analysis, basal values were averaged as were the 3 values immediately after oligomycin treatment and the 3 values at 1 h after oligomycin treatment.

For the 2-deoxy-<sup>3</sup>H-glucose uptake assay, mature brown adipocytes were cultivated overnight in serum-free medium and were stimulated with 1 μM CL 316, 243 (Sigma-Aldrich GmbH) (12) or distilled water followed by incubation at 37°C in 5% CO<sub>2</sub> for 110 min. Cells were washed once with prewarmed phosphate-buffered saline, then 2-deoxy-<sup>3</sup>H-glucose (0.5 kBq/mL) and 2-deoxy-glucose (100 μM) were added, followed by incubation at 37°C in 5% CO<sub>2</sub> for 10 min. After being washed with ice-cold phosphate-buffered saline, cells were lysed with radioimmunoprecipitation assay buffer and transferred to a liquid scintillation analyzer (PerkinElmer) for 3 h. Uptake rates of 2-deoxy-<sup>3</sup>H-glucose were normalized to protein concentration.

### Statistics

Two-way ANOVA with the Sidak post hoc test was used to assess differences between groups (GraphPad Software Inc.). *P* values of less than 0.05 were considered significant.

### RESULTS

The increase in whole-body oxygen consumption caused by CL 316, 243 treatment was blunted in UCP1 KO compared with WT mice ( $F_{1, 90} = 554.8$ ,  $P < 0.0001$ ) (Fig. 1A) as was the rise in core body temperature ( $F_{1, 35} = 10.77$ ,  $P = 0.0023$ ) (Fig. 1B).

Representative thermal images are presented in Figure 2A. Unlike UCP1 KO mice, WT mice showed an increase in interscapular BAT temperature in response to CL 316, 243 treatment ( $F_{1, 30} = 18.53$ ,  $P = 0.0002$ ) (Fig. 2B).

Representative <sup>18</sup>F-FDG PET/MRI data are presented in Figure 3A. Both WT and UCP1 KO mice showed an increased mean SUV for <sup>18</sup>F-FDG in BAT in response to CL 316, 243 treatment relative to vehicle treatment ( $P < 0.0001$ ) (Fig. 3B), with no significant effect of genotype found ( $F_{1, 14} = 0.17$ ,  $P = 0.68$ ).

Extracellular flux analysis of cultured primary brown adipocytes revealed that 1 h after oligomycin treatment, reporting induction of uncoupled respiration (13), oxygen consumption rates were significantly lower for UCP1 KO than WT cells ( $P < 0.001$ ) (Fig. 4A). In contrast, extracellular acidification rates, reporting glycolytic activity (13), tended to be similar between UCP1 KO and WT cells at this time point after oligomycin treatment ( $P = 0.07$ ) (Fig. 4B). Both WT and UCP1 KO brown adipocytes showed an increase in 2-deoxy-<sup>3</sup>H-glucose uptake in response to CL 316, 243 treatment compared with vehicle ( $P = 0.01$  and  $P < 0.0001$ , respectively) (Fig. 4C), with no significant effect of genotype found ( $F_{1, 12} = 0.00045$ ,  $P = 0.97$ ).

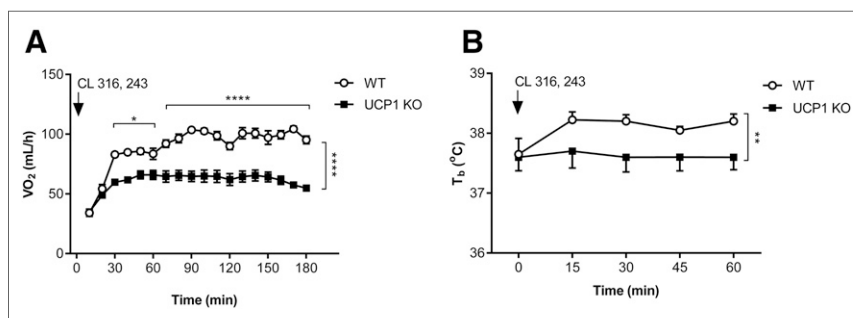


**FIGURE 1.** (A) Diminished oxygen consumption (VO<sub>2</sub>) and (B) core body temperature (T<sub>b</sub>) changes in response to adrenergic stimulation in UCP1 KO mice. Data points represent mean ± SEM of 3–5 animals per group. \**P* < 0.05. \*\**P* < 0.01. \*\*\*\**P* < 0.0001.

### DISCUSSION

The findings from the present study demonstrate that glucose metabolism can increase in brown adipocytes in the absence of UCP1-mediated uncoupled respiration and heat production.

In mouse primary brown adipocytes treated with CL 316,243, glucose is transported into the cell and through the action of diacylglycerol acyltransferase 2 feeds into specialized lipid droplet pools, which are simultaneously hydrolyzed (14). The released

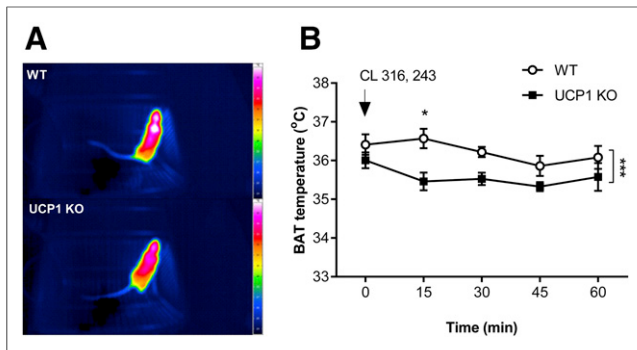


**FIGURE 2.** (A) Representative thermal images of WT (top) and UCP1 KO (bottom) mice taken 15 min after CL 316, 243 injections. (B) Defective BAT thermogenesis in response to adrenergic stimulation in UCP1 KO mice. Data points represent mean  $\pm$  SEM of 4 animals per group. \* $P < 0.05$ . \*\*\* $P < 0.001$ .

free fatty acids are then either rapidly oxidized or activate UCP1 in mitochondria (14). Our findings of similar  $\beta_3$  adrenergic receptor-stimulated  $^{18}\text{F}$ -FDG/2-deoxy- $^3\text{H}$ -glucose uptake between WT and UCP1 KO brown adipocytes suggest that UCP1 (thermogenic) function does not provide feedback, on the initial step at least, of this concerted process.

Noradrenaline treatment was previously found not to stimulate BAT 2-deoxy- $^3\text{H}$ -glucose uptake in male UCP1 KO mice (15). The discordance with the findings from the present study could be explained by our use of female UCP1 KO mice. Indeed, cold-stimulated BAT  $^{18}\text{F}$ -FDG uptake is diminished in male UCP1 KO mice but not in female counterparts (16).

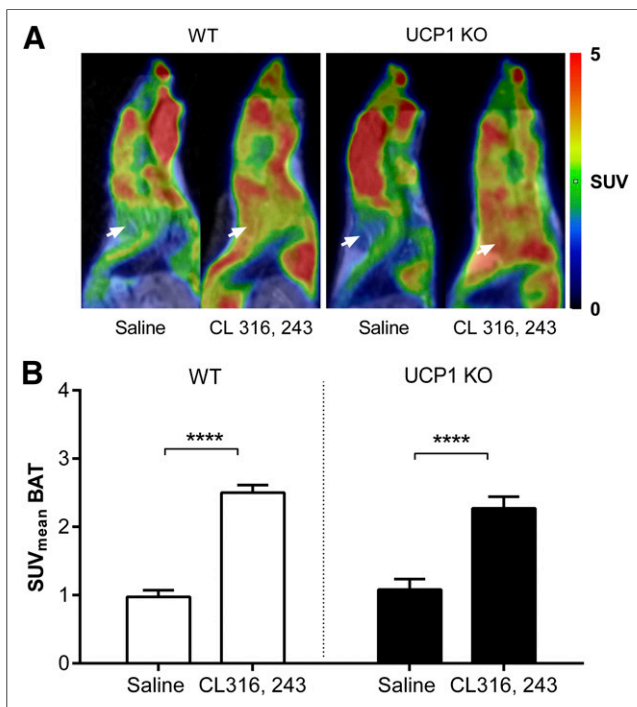


**FIGURE 3.** (A) Representative PET/MRI data of WT and UCP1 KO mice taken 45–60 min after CL 316, 243/saline and  $^{18}\text{F}$ -FDG injections. White arrows in each image point to interscapular BAT. (B) Retained BAT  $^{18}\text{F}$ -FDG uptake in response to adrenergic stimulation in UCP1 KO mice. Bars represent mean  $\pm$  SEM of 4–5 animals per group. \*\*\*\* $P < 0.0001$ .

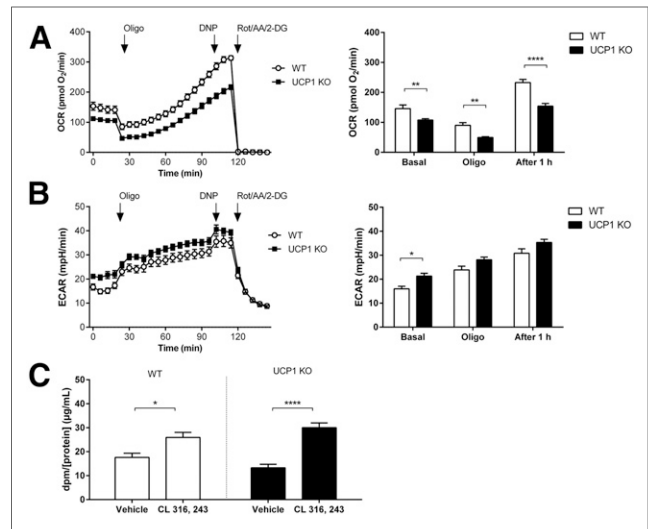


**FIGURE 4.** (A) Impaired induction of uncoupled respiration but normal (B) glycolysis and (C) 2-deoxy- $^3\text{H}$ -glucose uptake in UCP1 KO mouse primary brown adipocytes. Data points represent mean  $\pm$  SEM of 4–6 cultures per group. 2-DG = 2-deoxyglucose; AA = antimycin A; DNP = dinitrophenol; dpm = dose per minute; ECAR = extracellular acidification rate; Rot = rotenone. \* $P < 0.05$ . \*\* $P < 0.01$ . \*\*\*\* $P < 0.0001$ .

It is unlikely that the low BAT  $^{18}\text{F}$ -FDG uptake in the present study is diet related (17). This is because we found in preliminary experiments performed on high-fat high-sugar fed mice a much higher amount of BAT  $^{18}\text{F}$ -FDG uptake when animals were housed and scanned at room temperature ( $22^\circ\text{C}$ ). This suggests that experimental conditions even only mildly below thermoneutrality ( $30^\circ\text{C}$  for mice) (8) can significantly stimulate BAT. Therefore, studies under thermoneutral conditions are optimal because the low BAT activity constitutes a true basal state allowing the effects of novel stimulators of BAT to be examined in isolation.

## CONCLUSION

BAT  $^{18}\text{F}$ -FDG uptake and UCP1-mediated heat production can be dissociated. Additional techniques that measure BAT thermogenesis apart from  $^{18}\text{F}$ -FDG PET imaging and blood flow measurements (18) are required in model systems in which UCP1 is expected not to be functional. Because UCP1 deficiency is not the standard physiologic scenario in humans, caution is, however, warranted when translating our findings.

## DISCLOSURE

The work in this manuscript was funded by the German Federal Ministry of Education and Research, the German Research Foundation, and the German Centre for Diabetes Research. No other potential conflict of interest relevant to this article was reported.

## ACKNOWLEDGMENT

We thank Dr. Kerstin Krause for assistance with the experiments.

## REFERENCES

- van der Lans AA, Hoeks J, Brans B, et al. Cold acclimation recruits human brown fat and increases nonshivering thermogenesis. *J Clin Invest*. 2013;123:3395–3403.
- Virtanen KA, Lidell ME, Orava J, et al. Functional brown adipose tissue in healthy adults. *N Engl J Med*. 2009;360:1518–1525.
- Cypess AM, Weiner LS, Roberts-Toler C, et al. Activation of human brown adipose tissue by a  $\beta$ 3-adrenergic receptor agonist. *Cell Metab*. 2015;21:33–38.
- Cypess AM, Doyle AN, Sass CA, et al. Quantification of human and rodent brown adipose tissue function using  $^{99m}\text{Tc}$ -methoxyisobutylisonitrile SPECT/CT and  $^{18}\text{F}$ -FDG PET/CT. *J Nucl Med*. 2013;54:1896–1901.
- Fueger BJ, Czernin J, Hildebrandt I, et al. Impact of animal handling on the results of  $^{18}\text{F}$ -FDG PET studies in mice. *J Nucl Med*. 2006;47:999–1006.
- Porter C, Herndon DN, Chondronikola M, et al. Human and mouse brown adipose tissue mitochondria have comparable UCP1 function. *Cell Metab*. 2016;24:246–255.
- Inokuma K, Okamatsu-Ogura Y, Omachi A, et al. Indispensable role of mitochondrial UCP1 for antiobesity effect of beta3-adrenergic stimulation. *Am J Physiol Endocrinol Metab*. 2006;290:E1014–E1021.
- Feldmann HM, Golozoubova V, Cannon B, et al. UCP1 ablation induces obesity and abolishes diet-induced thermogenesis in mice exempt from thermal stress by living at thermoneutrality. *Cell Metab*. 2009;9:203–209.
- Crane JD, Mottillo EP, Farncombe TH, et al. A standardized infrared imaging technique that specifically detects UCP1-mediated thermogenesis in vivo. *Mol Metab*. 2014;3:490–494.
- Hankir MK, Kranz M, Gnad T, et al. A novel thermoregulatory role for PDE10A in mouse and human adipocytes. *EMBO Mol Med*. 2016;8:796–812.
- Fisher FM, Kleiner S, Douris N, et al. FGF21 regulates PGC-1 $\alpha$  and browning of white adipose tissues in adaptive thermogenesis. *Genes Dev*. 2012;26:271–281.
- Chernogubova E, Cannon B, Bengtsson T. Norepinephrine increases glucose transport in brown adipocytes via beta3-adrenoceptors through a cAMP, PKA, and PI3-kinase-dependent pathway stimulating conventional and novel PKCs. *Endocrinology*. 2004;145:269–280.
- Divakaruni AS, Paradyse A, Ferrick DA, et al. Analysis and interpretation of microplate-based oxygen consumption and pH data. *Methods Enzymol*. 2014;547:309–354.
- Irshad Z, Dimitri F, Christian M, et al. Diacylglycerol acyltransferase 2 (DGAT2) links glucose utilization to fatty acid oxidation in the brown adipocytes. *J Lip Res*. 2017;58:15–30.
- Inokuma K, Ogura-Okamatsu Y, Toda C, et al. Uncoupling protein 1 is necessary for norepinephrine-induced glucose utilization in brown adipose tissue. *Diabetes*. 2005;54:1385–1391.
- Jeanguillaume C, Metrard G, Ricquier D, et al. Visualization of activated BAT in mice, with FDG-PET and its relation to UCP1. *Adv J Mol Imaging*. 2013;3:19–22.
- Roberts-Toler C, O'Neill BT, Cypess AM. Diet-induced obesity causes insulin resistance in mouse brown adipose tissue. *Obesity (Silver Spring)*. 2015;23:1765–1770.
- Abreu-Vieira G, Hagberg CE, Spalding KL, et al. Adrenergically stimulated blood flow in brown adipose tissue is not dependent on thermogenesis. *Am J Physiol Endocrinol Metab*. 2015;308:E822–E829.



The Journal of  
NUCLEAR MEDICINE

## Dissociation Between Brown Adipose Tissue $^{18}\text{F}$ -FDG Uptake and Thermogenesis in Uncoupling Protein 1-Deficient Mice

Mohammed K. Hankir, Mathias Kranz, Susanne Keipert, Juliane Weiner, Sille G. Andreasen, Matthias Kern, Marianne Patt, Nora Klötting, John T. Heiker, Peter Brust, Swen Hesse, Martin Jastroch and Wiebke K. Fenske

*J Nucl Med.* 2017;58:1100-1103.  
Published online: January 12, 2017.  
Doi: 10.2967/jnumed.116.186460

---

This article and updated information are available at:  
<http://jnm.snmjournals.org/content/58/7/1100>

---

Information about reproducing figures, tables, or other portions of this article can be found online at:  
<http://jnm.snmjournals.org/site/misc/permission.xhtml>

Information about subscriptions to JNM can be found at:  
<http://jnm.snmjournals.org/site/subscriptions/online.xhtml>

*The Journal of Nuclear Medicine* is published monthly.  
SNMMI | Society of Nuclear Medicine and Molecular Imaging  
1850 Samuel Morse Drive, Reston, VA 20190.  
(Print ISSN: 0161-5505, Online ISSN: 2159-662X)

© Copyright 2017 SNMMI; all rights reserved.

The logo for the Society of Nuclear Medicine and Molecular Imaging (SNMMI) consists of the letters 'S', 'N', 'M', and 'I' arranged in a 2x2 grid. Each letter is white and set within a red square. To the right of this grid, the full name of the society is written in a sans-serif font: 'SOCIETY OF NUCLEAR MEDICINE AND MOLECULAR IMAGING'.

SOCIETY OF  
NUCLEAR MEDICINE  
AND MOLECULAR IMAGING